[1] a) P. J. Stang, B. Olenyuk, *Acc. Chem. Res.* **1997**, *30*, 502 – 518; b) *Comprehensive Supramolecular Chemistry, Vols. 1–11* (Eds.: J.-M. Lehn, J. L. Atwood, J. E. D. Davis, D. D. MacNicol, F. Vögtle),, Pergamon, Oxford, UK, **1996**; c) J.-M. Lehn, *Supramolecular Chemistry: Concepts and Perspectives*, VCH, Weinheim, **1995**.

[2] a) O. D. Fox, M. G. B. Drew, P. D. Beer, *Angew. Chem.* **2000**, *112*, 139 – 144; *Angew. Chem. Int. Ed.* **2000**, *39*, 135 – 140; b) T. Kusukawa, M. Fujita, *Angew. Chem.* **1998**, *110*, 3327 – 3329; *Angew. Chem. Int. Ed.* **1998**, *37*, 3142 – 3144; c) B. Olenyuk, J. A. Whiteford, A. Fechtenkotter, P. J. Stang, *Nature* **1999**, *398*, 796 – 799; d) A. Ikeda, M. Yoshimura, H. Udzu, C. Fukuhara, S. Shinkai, *J. Am. Chem. Soc.* **1999**, *121*, 4296 – 4297; e) P. Jacopozzi, E. Dalcanale, *Angew. Chem.* **1997**, *109*, 665 – 667; *Angew. Chem. Int. Ed. Engl.* **1997**, *36*, 613 – 615; f) R. W. Saalfrank, H. Glaser, B. Demleitner, F. Hampel, M. M. Chowdhry, V. Schünemann, A. X. Trautwein, G. B. M. Vaughan, R. Yeh, A. W. Davis, K. N. Raymond, *Chem. Eur. J.* **2002**, *8*, 493 – 497.

[3] a) V. W.-W. Yam, E. C.-C. Cheng, Z.-Y. Zhou, *Angew. Chem.* **2000**, *112*, 1749 – 1751; *Angew. Chem. Int. Ed.* **2000**, *39*, 1683 – 1685; b) F. A. Cotton, L. M. Daniels, C. Lin, C. A. Murillo, *Inorg. Chem. Commun.* **2001**, *4*, 130 – 133; c) G. A. van Albada, I. Mutikainen, U. Turpeinen, J. Reedijk, *Eur. J. Inorg. Chem.* **1998**, 547 – 549; d) G. Lowe, S. A. Ross, M. Probert, A. Cowley, *Chem. Commun.* **2001**, 1288 – 1289; e) F. J. Winkler, R. Medina, J. Winkler, H. Krause, *J. Mass Spectrom.* **1997**, *32*, 1072 – 1079.

[4] Chiral capsules based on hydrogen bonds: a) J. M. Rivera, T. Martín, J. Rebek, Jr.,*Science* **1998**, *279*, 1021 – 1023; b) L. J. Prins, J. Huskens, F. de Jong, P. Timmerman, D. N. Reinhoudt, *Nature* **1999**, *398*, 498 – 502; chiral capsules based on metal–ligand interactions: c) S. Hiraoka, M. Fujita, *J. Am. Chem. Soc.* **1999**, *121*, 10239 – 10240; d) A. J. Terpin, M. Ziegler, D. W. Johnson, K. N. Raymond, *Angew. Chem.* **2001**, *113*, 161 – 164; *Angew. Chem. Int. Ed.* **2001**, *40*, 157 – 160; circular helicates based on metal–ligand interactions: e) C. Provent, S. Hewage, G. Brand, G. Bernardinelli, L. J. Charbonnière, A. F. Williams, *Angew. Chem.* **1997**, *109*, 1346 – 1348; *Angew. Chem. Int. Ed. Engl.* **1997**, *36*, 1287 – 1289; f) C. Provent, E. Rivara-Minten, S. Hewage, G. Brunner, A. F. Williams, *Chem. Eur. J.* **1999**, *5*, 3487 – 3494; g) O. Mamula, A. von Zelewsky, G. Bernardinelli, *Angew. Chem.* **1998**, *110*, 302 – 305; *Angew. Chem. Int. Ed.* **1998**, *37*, 290 – 293; h) G. Baum, E. C. Constable, D. Fenske, C. E. Housecroft, T. Kulke, *Chem. Commun.* **1999**, 195 – 196.

[5] a) R. Kramer, J.-M. Lehn, A. Marquis-Rigault, *Proc. Natl. Acad. Sci. USA* **1993**, *90*, 5394 – 5398; b) B. Hasenknopf, J.-M. Lehn, G. Baum, D. Fenske, *Proc. Natl. Acad. Sci. USA* **1996**, *93*, 1397 – 1400; c) D. Caulder, K. N. Raymond, *Angew. Chem.* **1997**, *109*, 1508 – 1510; *Angew. Chem. Int. Ed. Engl.* **1997**, *36*, 1440 – 1442; d) M. Albrecht, M. Schneider, H. Röttele, *Angew. Chem.* **1999**, *111*, 512 – 515; *Angew. Chem. Int. Ed.* **1999**, *38*, 557 – 559; e) M. A. Masood, E. J. Enemark, T. D. P. Stack, *Angew. Chem.* **1998**, *110*, 973 – 977; *Angew. Chem. Int. Ed.* **1998**, *37*, 928 – 932; f) T. W. Kim, M. S. Lah, J.-I. Hong, *Chem. Commun.* **2001**, 743 – 744.

[6] Ligands were prepared according to the previous report: H.-J. Kim, Y.-H. Kim, J.-I. Hong, *Tetrahedron Lett.* **2001**, *42*, 5049 – 5052.

[7] $[Ag_3L_2^{*Me(S)}](NO_3)_3$ in the solid state has to be described as being composed of a cationic form, $[Ag_3L_2^{*Me(S)}(NO_3)_2(CH_3CN)_4]^+$, and an anionic form, $[Ag_3L_2^{*Me(S)}(NO_3)_4(CH_3CN)_2]^-$. Crystal structure of $\{(M)$-$[Ag_3L_2^{*Me(S)}(CH_3CN)_4(NO_3)_2]\}\{(M)$-$[Ag_3L_2^{*Me(S)}(CH_3CN)_2(NO_3)_4]\}$: $C_{42}H_{51}Ag_3N_{12}O_{15}$, $M_w = 1287.56$, colorless crystal, $0.45 \times 0.38 \times 0.20$ mm^3, monoclinic $C2$, $a = 23.7463(13)$, $b = 14.1186(8)$, $c = 15.3235(9)$ Å; $\alpha = 90$, $\beta = 97.503(1)$, $\gamma = 90°$; $V = 5093.4(5)$ Å^3, $Z = 4$, $\rho_{calcd} = 1.679$ Mg m^{-3}(including solvent), $\mu(Mo_{K\alpha})$, $\lambda = 0.71073$ Å) $= 1.219$ mm^{-1}, $2\theta_{max} = 56.56°$; 15905 measured reflections, of which 11383 were unique. The structure was solved by direct methods and refined by full-matrix least squares calculations with SHELX-97. The final $R1 = 0.0245$, $wR2 = 0.0557$ ($I > 2\sigma(I)$); $R1 = 0.0278$, $wR2 = 0.0572$ (all data); measurements: Siemens SMART CCD equipped with a graphite crystal incident-beam monochromator *L*p. CCDC-182210 contains the supplementary crystallographic data for this paper. These data can be obtained free of charge via www.ccdc.cam.ac.uk/conts/retrieving.html (or from the Cambridge Crystallographic Data Centre, 12, Union Road, Cambridge CB2 1EZ, UK; fax: (+44) 1223-336-033; or deposit@ccdc.cam.ac.uk).

[8] W. L. Jörgensen, D. L. Severance, *J. Am. Chem. Soc.* **1990**, *112*, 4768 – 4774.

[9] Although the right-handed model structure of (P)-$[Ag_3L_2^{*Me(S)}]^{3+}$ is desirable for comparison with a left-handed X-ray crystal structure of (M)-$[Ag_3L_2^{*Me(S)}]^{3+}$, the right-handed structure was not available due to the perturbed rotation along the C_3 helical axis in (M)-$[Ag_3L_2^{*Me(S)}]^{3+}$. Instead, a model structure of (M)-$[Ag_3L_2^{*Me(R)}]^{3+}$ energetically equivalent to (P)-$[Ag_3L_2^{*Me(S)}]^{3+}$ was obtained by simple chirality inversion in the ligands from the solid structure of (M)-$[Ag_3L_2^{*Me(S)}]^{3+}$ and compared with the solid structure; MacroModel 7.0 with modified MM2 force field. F. Mohamadi, N. G. J. Richards, W. C. Guida, R. Liskamp, M. Lipton, C. Caufield, G. Chang, T. Hendrickson, W. C. Still, *J. Comput. Chem.* **1990**, *11*, 440.

[10] Crystal structure of (M)-$[Ag_3L_2^{*Me(S)}(CH_3CN)_2(NO_3)_3]/(P)$-$[Ag_3L_2^{*Me(R)}(CH_3CN)_2(NO_3)_3]$: $C_{40}H_{48}Ag_3N_{11}O_{15}$, $M_w = 1246.50$, colorless crystal $0.45 \times 0.38 \times 0.20$ mm^3, monoclinic $C2/c$, $a = 24.408(3)$, $b = 14.0353(17)$, $c = 14.1561(17)$ Å; $\alpha = 90$, $\beta = 96.760(2)$, $\gamma = 90°$; $V = 4815.7(10)$ Å^3, $Z = 4$, $\rho_{calcd} = 1.719$ Mg m^{-3}(including solvent), $\mu(Mo_{K\alpha})$, $\lambda = 0.71073$ Å) $= 1.285$ mm^{-1}, $2\theta_{max} = 56.56°$; 14328 measured reflections, of which 5623 were unique. The structure was solved by direct methods and refined by full-matrix least squares calculations with SHELX-97. The final $R1 = 0.0468$, $wR2 = 0.0963$ ($I > 2\sigma(I)$); $R1 = 0.1016$, $wR2 = 0.1154$ (all data); measurements: Siemens SMART CCD equipped with a graphite crystal incident-beam monochromator *L*p. CCDC-182211 contains the supplementary crystallographic data for this paper. These data can be obtained free of charge via www.ccdc.cam.ac.uk/conts/retrieving.html (or from the Cambridge Crystallographic Data Centre, 12, Union Road, Cambridge CB2 1EZ, UK; fax: (+44) 1223-336-033; or deposit@ccdc.cam.ac.uk).

[11] m/z 1290.0 of $[Ag_3L^{*Ph(S)}L^{*Me(S)}(NO_3)_2]^+$ and 1308.0 of $[Ag_3L^{*Ph(S)}L^{*Me(S)}(NO_3)_2(H_2O)]^+$.

Deracemization of α-Methylbenzylamine Using an Enzyme Obtained by In Vitro Evolution**

Marina Alexeeva, Alexis Enright, Michael J. Dawson, Mahmoud Mahmoudian, and Nicholas J. Turner*

Enantiomerically pure chiral amines are valuable synthetic intermediates, particularly for the preparation of pharmaceutical compounds. Traditionally, chiral amines have been obtained by resolution-based procedures, for example, by kinetic resolution of a racemate using an enzyme[1,2] or crystallization of a diastereomer using a chiral acid to form a salt.[3] Increasingly, there is a desire to develop asymmetric approaches, or their equivalents, which can in principal deliver the product in 100 % yield and 100 % *ee*. For example, transaminases have been utilized for the conversion of

[*] Prof. N. J. Turner, M. Alexeeva, A. Enright
Department of Chemistry
Centre for Protein Technology, The University of Edinburgh
King's Buildings, West Mains Road, Edinburgh EH9 3JJ (UK)
Fax: (+44) 131-650-4717
E-mail: n.j.turner@ed.ac.uk
Dr. M. J. Dawson, Dr. M. Mahmoudian
GlaxoSmithKline R&D, Medicines Research Centre
Gunnels Wood Road, Stevenage, Hertfordshire, SG1 2NY, (UK)

[**] We are grateful to the BBSRC and GlaxoSmithKline for funding a postdoctoral fellowship (M.A.) and CASE award (A.E.). We also thank the Wellcome Trust for financial support.

ketones into chiral amines[4] and chiral ruthenium catalysts have been used for the asymmetric reduction of imines.[5] Alternative strategies are based upon the dynamic kinetic resolution of amines, for example, by using *Burkholderia plantarii* lipase[6] or *Candida antarctica* lipase[7] with appropriate in situ racemization protocols.

Recently we described a method for the deracemization of a range of α-amino acids that gave high yields and optical purities[8,9] (Scheme 1, $R^2 = CO_2H$). This deracemization method involves the stereoinversion of one enantiomer to the other by repeated cycles of enzyme-catalyzed oxidation to

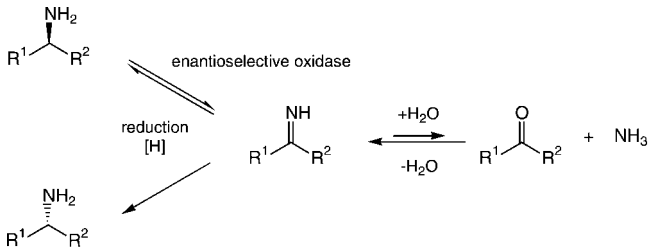

Scheme 1. Process for the deracemization of chiral amines by employing a cyclic sequence of enantioselective oxidation using an amine oxidase coupled with a nonselective reducing agent.

the imine, followed by nonselective reduction back to the amino acid.[10] We demonstrated that both L- and D-α-amino acids can be prepared in this way by employing enantioselective D-[8] and L-amino acid oxidases,[9] respectively. A key factor that determines the efficiency of the deracemization process is the choice of reducing agent. In the early reports[11] sodium borohydride was employed, although the instability of this reagent at pH 7 precludes its use on a practical scale. However, this problem can be overcome by switching to alternative, stable reductants such as sodium cyanoborohydride,[8] ammonium formate with Pd/C,[9] and also amine–borane complexes.[9] Herein we report a significant new extension of the deracemization strategy by applying the method for the first time to the deracemization of chiral amines.[12]

The key issue at the outset was the identification of enantioselective amine oxidases that would be suitable for the oxidation-reduction cycle. Amine oxidases have been classified into two groups, namely, Type I (Cu/TOPA-dependent) and Type II (flavin-dependent).[13] In the catalytic cycle of the Type I enzyme the intermediate imine remains covalently bound to the protein and hence these enzymes were deemed unsuitable for our use. The Type II enzymes generate "free" imines, and although they are well known from mammalian sources,[14] their microbial counterparts are poorly documented; indeed at the outset of this work there were no reports of enantioselective transformations. Schilling and Lerch[15] reported the cloning and expression of a Type II monoamine oxidase from *Aspergillus niger* (MAO-N), and Sablin et al.[16] subsequently purified the enzyme to homogeneity and carried out substrate-specificity and kinetic studies. The enzyme was reported to have high activity towards simple aliphatic amines (for example, amylamine, butylamine) but was also active, albeit at a lower rate, towards benzylamine. We decided to select α-methylbenzylamine (AMBA, Scheme 1, $R^1 = Ph$, $R^2 = Me$) as a model system for study in view of its importance as a chiral amine.[6] Our initial studies revealed that the *A. niger* MAO-N enzyme possessed very low, but measurable, activity towards L-α-methylbenzylamine and even slower oxidation of the D enantiomer (see below). We reasoned that such activity represented a viable starting point for improvement of both the catalytic activity and enantioselectivity using in vitro evolution methods.[17]

The MAO-N gene from *A. niger* was obtained from Schilling and Lerch[15] and subcloned into the *E. coli* PET16b vector. Sequencing of the gene revealed four differences in the amino acid sequence compared to the published sequence (A300V, L304V, K348M, and R450G). Two of these differences (K348M and R450G) had previously been noted by Sablin et al.[16] However, the activity of the enzyme (see below) was found to be comparable to published data and hence we used this plasmid as the starting point for the in vitro evolution experiments. The initial priority was the development of an effective high-throughput screen for amine oxidase activity and, in this respect, we focussed on a method that would allow approximately 2000–3000 colonies per plate to be visualized. Amine oxidases are typical of all members of the oxidase family in that they evolve hydrogen peroxide as a by-product. Many of the reported assays for oxidase activity are based upon capture of the peroxide by a peroxidase in the presence of a substrate that yields a highly colored product upon oxidation. Use of 3,3′-diaminobenzidine (DAB) as the peroxidase substrate gave rise to a dark pink, insoluble product that gave both very high definition and contrast of the active colonies (Figure 1).

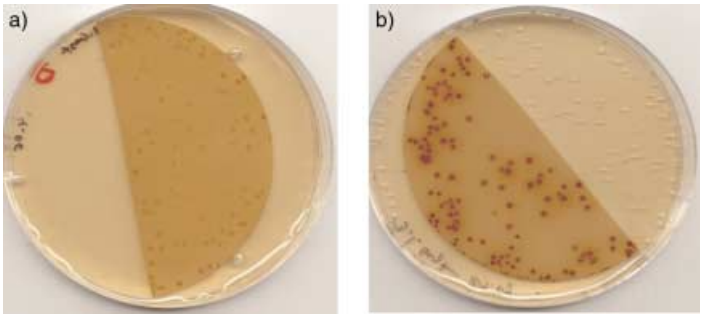

Figure 1. Colorometric plate based screening assay for amine oxidase activity by capture of the hydrogen peroxide produced using 3,3′-diaminobenzidine with peroxidase: a) colonies with D-α-methylbenzylamine and b) identical clones with the L enantiomer.

The library of variants was generated by carrying out multiple cycles of mutagenesis using the *E. coli* XL1-Red mutator strain[18] followed by transformation of the plasmid library into *E. coli* BL21. The library was plated out directly onto nitrocellulose filters on agar plates (ca. 3000 colonies per plate) and, following partial lysis of the cells, each plate was treated with a cocktail containing both the assay mixture (L- or D-AMBA, DAB) and also 2% agarose. The plates were incubated at 37 °C after which they were inspected for positive clones. By using this colorometric assay we were able to identify clones that possessed higher activity towards L-AMBA than the D enantiomer (Figure 1).

  0044-8249/02/11417-3310 $ 20.00+.50/0 *Angew. Chem.* **2002**, *114*, Nr. 17

The result of screening a subset (ca. 150000 clones) of the library led to the identification of 35 clones with improved activity towards L-AMBA compared to the wild-type enzyme. Each of these clones was grown on a small scale and assayed against both L- and D-AMBA as cell-free extracts, which resulted in the best 27 clones being selected for further study. Each of these 27 clones was assayed against amylamine, L-AMBA, and D-AMBA (Figure 2).

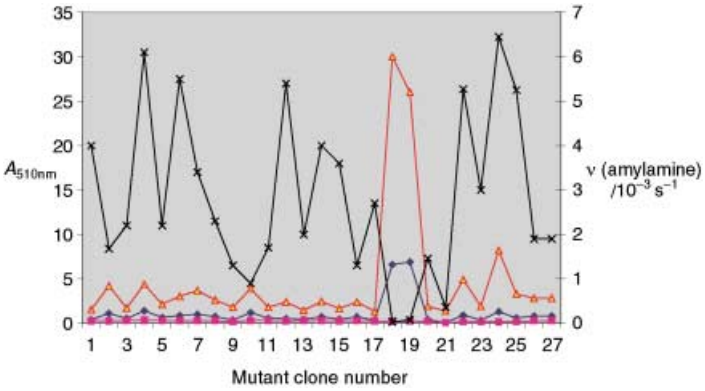

Figure 2. Activity of the best 27 clones identified from screening ca. 150000 colonies. Blue line: L-AMBA as substrate, pink: D-AMBA, orange: ratio of activity towards L- versus D-AMBA, black: amylamine. The left-hand *y* axis corresponds to absorption data (recorded at 510 nm) for L-AMBA, D-AMBA, and the ratio of L/D-AMBA. The absorbance was recorded after incubation for 96 h. The right-hand *y* axis corresponds to data for amylamine. Initial rates were measured.

Examination of the polyacrylamide gels showed that several of these 27 clones appeared to be "expression mutants", as evidenced by increased levels of protein expression. However two (identical) clones were clearly superior in terms of their selectivity and activity towards L- versus D-AMBA and appeared not to have increased levels of expression of MAO-N. This clone was therefore selected for more detailed examination.

Both the wild-type and mutant MAO-N were purified by a modification of the literature procedure to give protein of approximately 10% purity. Each enzyme was then assayed against L-AMBA, D-AMBA, benzylamine, and amylamine as the substrate (Table 1).

The data revealed that the activity of the mutant towards L-AMBA ($k_{cat} = 8.0\ min^{-1}$) was 47-fold higher than the wild-type enzyme ($k_{cat} = 0.17\ min^{-1}$). Moreover, the selectivity of the mutant for the L enantiomer versus D-AMBA (ca. 100:1) had also increased (5.8-fold) relative to the wild-type enzyme (ca. 17:1). Thus, the outcome of the in vitro evolution experiments had been to simultaneously improve both the enantioselectivity and catalytic activity of the enzyme. For comparison, the activity towards the best substrate for the wild-type enzyme, namely amylamine, and also benzylamine, is presented. Sequencing of the mutant revealed a single change in the amino acid sequence (Asn336Ser).

Table 1. K_m and k_{cat} values for wild-type and best mutant monoamine oxidase enzymes using L-AMBA, D-AMBA, benzylamine, and amylamine as substrates.

Substrate	Wild-type		Mutant	
	K_m[a] [mM]	k_{cat} [min^{-1}]	K_m [mM]	k_{cat} [min^{-1}]
L-AMBA	ND	0.17	0.4	8.0
D-AMBA	ND	0.01	ND[a]	0.08
benzylamine	ND	371	ND[a]	196
amylamine	ND	1000	0.4	116

[a] ND = not determined.

The substantial improvement in activity and selectivity of the mutant was confirmed by chiral HPLC (Chiralcel CrownPak CR+) in which complete oxidation of the L enantiomer was apparent after 24 h, whereas there was no detectable conversion of the D enantiomer. The final objective became the application of the mutant enzyme to the deracemization of DL-AMBA. A range of reducing agents was screened (sodium borohydride, catalytic transfer hydrogenation, amine–borane complexes) using 1 mM DL-AMBA as the substrate in the presence of the mutant MAO-N. This screen identified the ammonia–borane complex as the optimal reagent which gave a 77% yield of D-AMBA with an *ee* value of 93%. Greater optical purities of the product (up to 99% *ee*) could be achieved although at the expense of yield. We also carried out the stereoinversion of L- to D-AMBA (18% yield, 99% *ee*) and showed that under identical conditions there was no conversion of D- into L-AMBA.

In conclusion we have successfully achieved the "directed evolution" of an enzyme to meet the specific requirements of a novel biotransformation. The decision to select the *A. niger* MAO-N gene for in vitro evolution was based upon the observation that the wild-type MAO-N enzyme showed inherent selectivity for L- over D-AMBA (ca. 17:1), although the overall rate was very low. An interesting aspect of the present work is the identification of a mutant with enhanced enantioselectivity by using a single enantiomer substrate in the screen (L-AMBA). There is currently much effort directed towards the development of truly enantioselective screens in which racemates are used, thereby mimicking the real-life situation found in a kinetic resolution in which the two enantiomers compete for the enzyme.[19] It may be that if one is able to screen large enough libraries of variant genes (ca. 10^6), by using inherently simpler screens, then enzymes with improved enantioselectivity can be identified in the manner described here.

Received: April 4, 2002 [Z19043]

[1] A. Schmid, J. S. Dordick, B. Hauer, A. Kiener, M. Wubbolts, B. Witholt, *Nature* **2001**, *409*, 258; *Enzyme Catalysis in Organic Synthesis*, 2nd ed. (Eds.: K.-H. Drauz, H. Waldmann), Wiley-VCH, Weinheim, **2002**.

[2] S. Takayama, S. T. Lee, S. C. Hung, C.-H. Wong, *Chem. Commun.* **1999**, 127; D. T. Guranda, L. M. van Langen, F. van Rantwijk, R. A. Sheldon, V. K. Svedas, *Tetrahedron: Asymmetry* **2001**, *12*, 1645; L. M. Langen, N. H. P. Oosthoek, D. T. Guranda, F. van Rantwijk, V. K. Svedas, R. A. Sheldon, *Tetrahedron: Asymmetry* **2000**, *11*, 4593; L. E. Iglesias, V. M. Sanchez, F. Rebolledo, V. Gotor, *Tetrahedron: Asymmetry* **1997**, *8*, 2675.

[3] J. Balint, G. Egri, M. Czugler, J. Schindler, V. Kiss, Z. Juvancz, E. Fogassy, *Tetrahedron: Asymmetry* **2001**, *12*, 1511.

[4] J. S. Shin, B. G. Kim, A. Liese, C. Wandrey, *Biotechnol. Bioeng.* **2001**, *73*, 179; G. Matcham, M. Bhatia, W. Lang, C. Lewis, R. Nelson, A. Wang, W. Wu, *Chimia* **1999**, *53*, 584; J. S. Shin, B. G. Kim, *Biotechnol. Bioeng.* **1999**, *65*, 206.

  0044-8249/02/11417-3311 $ 20.00+.50/0

[5] N. Uematsu, A. Fujii, S. Hashiguchi, T. Ikariya, R. Noyori, *J. Am. Chem. Soc.* **1996**, *118*, 4916; J. Okuda, S. Verch, R. Sturmer, T. P. Spaniol, *J. Organomet. Chem.* **2000**, *605*, 55.
[6] G. Hieber, K. Ditrich, *Chimica Oggi* **2001**, *19*, 16; F. Balkenhohl, K. Ditrich, B. Hauer, W. Ladner, *J. Prakt. Chem.* **1997**, *339*, 381.
[7] M. T. Reetz, K. Schimossek, *Chimia* **1996**, *50*, 668; Y. K. Choi, M. J. Kim, Y. Ahn, M. J. Kim, *Org. Lett.* **2001**, *3*, 4099.
[8] T. Beard, N. J. Turner, *Chem. Commun.* **2002**, 246.
[9] F.-R. Alexandre, D. P. Pantaleone, P. P. Taylor, I. G. Fotheringham, D. J. Ager, N. J. Turner, *Tetrahedron Lett.* **2002**, *43*, 707.
[10] For recent reviews on the kinetics and stereochemistry of deracemization reactions, see U. T. Strauss, U. Felfer, K. Faber, *Tetrahedron: Asymmetry* **1999**, *10*, 107; K. Faber, *Chem. Eur. J.* **2001**, *7*, 5005.
[11] E. W. Hafner, D. Wellner, *Proc. Natl. Acad. Sci. USA* **1971**, *68*, 987; J. W. Huh, K. Yokoigawa, N. Esaki, K. Soda, *J. Ferment. Bioeng.* **1992**, *74*, 189; J. W. Huh, K. Yokoigawa, N. Esaki, K. Soda, *Biosci. Biotechnol. Biochem.* **1992**, *56*, 2081.
[12] For an example of the deracemization of chiral alcohols, see K. Soda, T. Oikawa, K. Yokoigawa, *J. Mol. Catal. B* **2001**, *11*, 149.
[13] P. L. Dostert, M. S. Benedetti, K. F. Tipton, *Med. Res. Rev.* **1989**, *9*, 45.
[14] R. B. Silverman, J. M. Cesarone, X. Liu, *J. Am. Chem. Soc.* **1993**, *115*, 4955.
[15] B. Schilling, K. Lerch, *Biochim. Biophys. Acta.* **1995**, *1243*, 529; B. Schilling, K. Lerch, *Mol. Gen. Genet.* **1995**, *247*, 430. We are grateful to Professor Schilling for the gift of the plasmid.
[16] S. O. Sablin, V. Yankovskaya, S. Bernard, C. N. Cronin, T. P. Singer, *Eur. J. Biochem.* **1998**, *253*, 270.
[17] *Directed Molecular Evolution of Proteins* (Eds.: S. Brakmann, K. Johnsson), Wiley-VCH, Weinheim, **2002**; D. Zha, S. Wilensek, M. Hermes, K.-E. Jaeger, M. T. Reetz, *Chem. Commun.* **2001**, 2664; E. T. Farinas, T. Bulter, F. H. Arnold, *Curr. Opin. Biotechnol.* **2001**, *12*, 545; J. D. Sutherland, *Curr. Opin. Chem. Biol.* **2000**, *4*, 263.
[18] A. Greener, M. Callahan, B. Jerpseth, *Mol. Biotechnol.* **1997**, *7*, 189; U. T. Bornscheuer, J. Altenbuchner, H. H. Meyer, *Bioorg. Med. Chem.* **1999**, *7*, 2169.
[19] M. T. Reetz, *Angew. Chem.* **2001**, *113*, 292; *Angew. Chem. Int. Ed.* **2001**, *40*, 284; J.-L. Reymond, *Chimia* **2001**, *55*, 1049; M. Baumann, R. Stürmer, U. T. Bornscheuer, *Angew. Chem.* **2001**, *113*, 4329; *Angew. Chem. Int. Ed.* **2001**, *40*, 4201.

Fabrication of Carbohydrate Chips for Studying Protein–Carbohydrate Interactions**

Sungjin Park and Injae Shin*

Carbohydrates play a central role in living organisms as recognition markers to enable cell adhesion, fertilization, differentiation, development, and tumor-cell metastasis through carbohydrate–protein interactions.[1] Interestingly, it is through these biomolecular interactions that bacteria and viruses adhere to the host cells and confer pathogenic properties.[1] Therefore, it is important to determine the molecular basis for specific protein–carbohydrate recognition events. Details of carbohydrate–protein interactions have been investigated mainly by biophysical and biochemical approaches, including X-ray crystallography and NMR spectroscopic studies of carbohydrate–protein complexes, mutagenesis, and synthesis of nonnatural sugar analogues.[2] Despite the established approaches to investigate carbohydrate–protein interactions, high-throughput methods have not been developed.

In the last decade, biological microchips (biochips) have been fabricated for a variety of applications. For instance, DNA chips (gene chips) are extensively used for tracking the activity of many genes at once and for studying changes in gene expression in diseased states.[3] Additionally, protein chips have been exploited for the high-throughput study of molecular interactions and biochemical activities,[4,5] and profiling protein expression in normal and diseased states.[6] Ziauddin and Sabatini have developed cell microarrays for the functional analysis of gene products in parallel.[7] Analogously, carbohydrate-based arrays may provide a new tool for the high-throughput study of carbohydrate–protein interactions.[8]

In many cases, carbohydrate-binding proteins recognize terminal and/or penultimate saccharides. Furthermore, they exhibit a strong affinity for multivalent carbohydrates with suitable spacing and orientation (cluster effect) but bind to monovalent oligosaccharides weakly.[9] Thus, we reasoned that carbohydrate chips that contain immobilized mono- and disaccharides with suitable distances between the carbohydrate probes on the glass surface could provide a useful tool for elucidating recognition events between carbohydrates and proteins at a molecular level.

An efficient immobilization technique of carbohydrates on the surface is essential for successful fabrication of carbohydrate chips. Recently, we prepared glycopeptides/glycoproteins by chemoselective ligation of maleimide-linked sugars to cysteine-possessing peptides/proteins.[10,11] Herein we report how this method was applied to immobilize carbohydrates on glass microscope slides (7.5 cm × 2.5 cm). As shown in Scheme 1, maleimide-linked sugars are attached through stable thioether linkages to the slide coated with thiol groups.

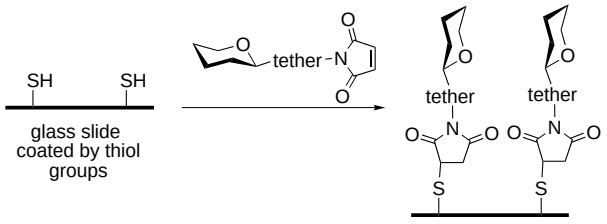

Scheme 1. Immobilization of maleimide-linked carbohydrates on thiol-derivatized slides.

Carbohydrates were appended to linkers L*n* of various lengths (L1, L2, L3, and L4) by coupling glycosylamines obtained from one-pot amination of carbohydrates to bifunctional cross-linkers such as **1** (Schemes 2 and 3).[10] Furthermore, we also prepared L2-NH_2 and L4-NH_2, which lack the carbohydrate moiety, to examine the nonspecific binding of lectins to linkers (Scheme 2).

[*] Prof. Dr. I. Shin, S. Park
Department of Chemistry, Yonsei University
Seoul 120-749 (Korea)
Fax: (+82) 2-364-7050
E-mail: injae@yonsei.ac.kr

[**] This work was supported by a grant from the Center for Integrated Molecular Systems (KOSEF). We thank Dr. Srikanth Dakoji (University of California, San Francisco) for his critical reading of the manuscript.

  0044-8249/02/11417-3312 $ 20.00+.50/0